4th MASHCON, Hamburg - Uliczka et al. (eds) - © 2016 Bundesanstalt für Wasserbau ISBN 978-3-939230-38-0 (Online)
DOI: 10.18451/978-3-939230-38-0_3

INTERACTION BETWEEN SHIP-INDUCED STRESS AND ASSOCIATED CHARACTERISTICS OF TURBIDITY RECORDS

S Niehueser, M Ulm, A Arns, J Jensen and **V Kelln**, Research Institute for Water and Environment, University of Siegen, Germany
K Uliczka and **B Kondziella**, Federal Waterways Engineering and Research Institute, Germany

SUMMARY

In a joint research project between the German Federal Waterways Engineering and Research Institute and the Research Institute for Water and Environment of the University of Siegen the ship-induced sediment transport as a proportion of the totally transported volume is investigated. Therefore, a field campaign in the Kiel Canal was conducted in 2012 and ship-induced loads were recorded. This paper highlights the preliminary results from analyzing the observed variables. First independent samples of observed passages were created and used to calculate correlations between the individual parameters. In a next step, high frequency turbidity records were separated into a common signal and linked to a critical sediment grain diameter. This procedure led to a classification depending on the ship-induced flow velocities because common characteristics of the turbidity measurements could be found. For further analyses the groups could be associated with AIS-transmitted parameters.

1 INTRODUCTION

Foreign trade is a vitally important factor in most economies. In Germany, inland navigation accounted for approximately 230 million tons of transported goods in 2014 (www.destatis.de, German Federal Statistical Office) indicating the demand for a robust and reliable transport infrastructure. However, both natural effects and anthropogenic interventions can cause sediment deposits in shipping channels and harbors which need to be dredged to maintain the infrastructures main function. Over the last decades, sediment dynamics have extensively been studied and a comprehensive review particularly dealing with transport issues in the San Francisco Bay Coastal System is provided in [1].
Sediment transport is generally described having extraordinary complex physical characteristics. The reason for that is the variety of parameters which directly influence the process [2]. Examples are the high turbulent hydrodynamical conditions as well as the sediment itself with different densities, shapes, grain diameters, grain size distributions, and storage conditions. Taking all these factors into account highlights that sediment transport is governed by quickly changing conditions in every time step. Another key challenge in this context is to quantify the amount of sediment deposit which is directly induced by the ship's passage and how the consequent sediment transport can be described as a function of the ship-induced load. The ship-induced load can be described e.g. by waves caused by the ship's passage, hereafter referred to as ship waves.
Investigations on ship waves are usually based on one of the following three methods: A first method is to perform expensive field measurements including all relevant processes as e.g. turbulences and other predominant conditions as e.g. tidal influences (e.g. [3], [4], [5], [6], [7], [29]). A second method for calculating the ship-induced waves is setting up a computational fluid dynamics (CFD) model (e.g. [8]) or using Boussinesq-type equations (e.g. [9], [10]). Such models are generally restricted by the underlying boundary conditions (e.g. ship's hull, inlet/outlet conditions). A third method is to rely on laboratory data of ship waves recorded in physical model experiments but these are limited to certain vessel types and waterway conditions [11]. Outcomes based on all three methods are often empirical formulas for describing wave parameters as e.g. the significant wave height but these formulas are usually only valid within a pre-defined range (e.g. [12], [13]). Furthermore, such empirical formulas are widely used for the calibration and validation of field measurements or numerical models (e.g. [11], [14], [29]).
In general, when moving along a waterway, a vessel usually generates a typical wave pattern which is divided into primary and secondary components (e.g. [15], [16], [11], [17]). The long-period primary wave is reflected alongside the ship and causes a fluctuation of the water level. These fluctuations are caused by the pressure and velocity distribution along the ship's hull showing pressure increases at the bow and stern and decreased pressure alongside of the ship. Consequently, rising water levels are found at the bow and stern (bow and stern wave) and a decreasing water level along the ships' side (drawdown). The drawdown corresponds to a reverse flow from the bow to the stern of the ship.
Replacement processes caused by the different pressure conditions induce the short-period secondary wave system. This system is mainly characterized by divergent and transverse waves (Kelvin waves) travelling away from both sides of the ship's hull with the ridges at an angle of 19.47° to the vessel's moving direction. The predominant contribution to the entire water level fluctuation can either originate from the primary or from the secondary wave system but depending on the waterway conditions. The primary waves prevail in restricted waterways while the secondary wave systems are more influential in unrestricted waterways [15].
In a joint research project the German Federal Waterways Engineering and Research Institute (BAW) and the Research Institute for Water and Environment (fwu) of

the University of Siegen aim at determining the ship-induced sediment transport as a proportion of the total volume transported in a tidal estuary [18]. Here, preliminary results are introduced, linking turbidity records with ship characteristics (e.g. geometry) and ship-induced stress (e.g. ship wave) using observational data from a field campaign that covers a large number of ship passages. The measurements were conducted at one specific cross-section of the Kiel Canal located in northern Germany and include but are not limited to turbidity records as well as geometries and velocities of and nearby the ships. Due to the limitation to stationary measurements this paper focusses on the aspect of sediment entrainment. Conclusions about the suspended sediment concentration in the entire water column or the sediment transport itself cannot be drawn directly.
However, the intention of this paper is to describe the interaction between ship and waterway with regard to the entire system and not for individual vessels.

2 STUDY AREA

The Kiel Canal is the most frequented artificial waterway in the world and has a total length of about 100 km connecting Brunsbüttel at the tidal Elbe River with Kiel at the Baltic Sea (see Figure 1) (e.g. [19], [20]). This artificial waterway reduces the route between the German North Sea and the Baltic Sea by nearly 450 km and the ships can avoid travelling all around northern Denmark.

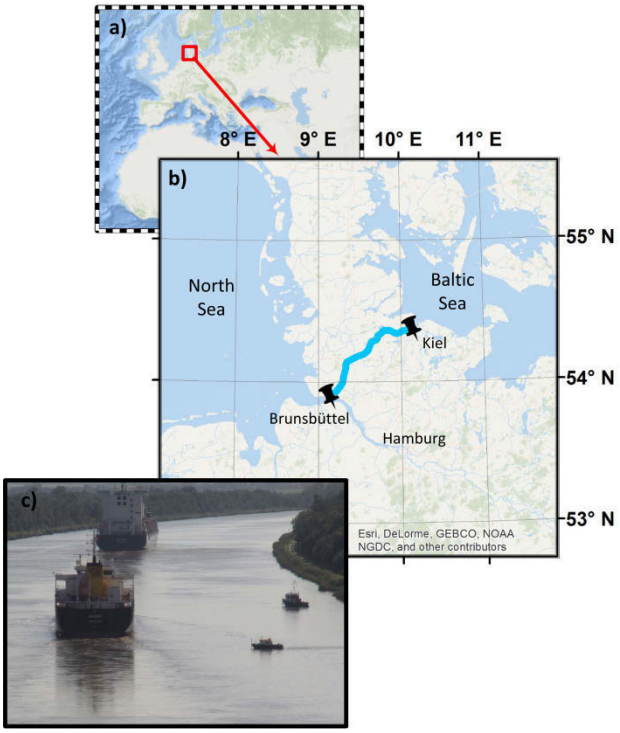

Figure 1. The Kiel Canal and a picture of the selected cross section during the field campaign (Photo: BAW).

In September 2012, the BAW carried out a field campaign in the Kiel Canal covering a period of approximately one week. The selected cross section is located at km 17.925 (near Brunsbüttel). In 2012 ~35,000 vessels passed through the Kiel Canal, i.e. more traffic than e.g. in the Suez Canal (http://www.wsa-kiel.wsv.de/Nord-Ostsee-Kanal/).
The Kiel Canal provides very constant and assessable conditions and is neither affected by tides nor strong currents (mostly from drainage processes). This very specific study site can thus be considered as field laboratory, one of the main reasons for selecting it for the field campaign.

3 DATA

The above mentioned measuring campaign provides both measurements at the bottom of the Kiel Canal as well as in the total water column by means of ship-based methods. Here, the focus is on stationary measurements at the bottom of the cross section. Figure 2 (top) shows the positions of the probes in the cross section having distances from the south bank as follows: 43.31 m (probe 1), 66.61 m (probe 2), and 82.85 m (probe 3).

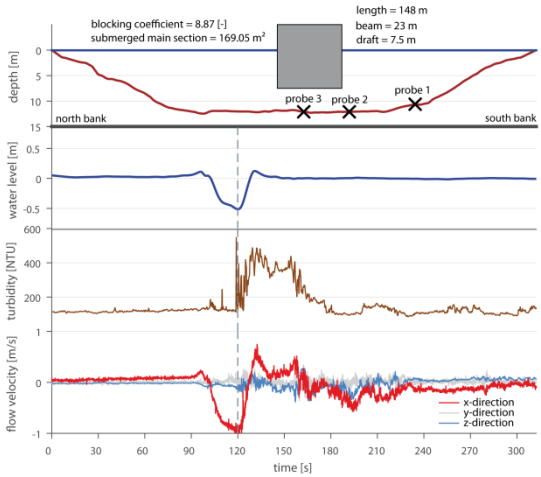

Figure 2. Overview of the recorded and investigated parameter (from top to bottom: idealized ship geometry and location of the probes, water level fluctuation, turbidity, flow velocity).

For the investigations different parameters were processed including water level, ship-induced flow velocities at the bottom (three-dimensional, recorded as x, y, z components) and turbidity information. Temporal resolutions are different for individual parameters with 8 Hz for the CTD probe (Conductivity, Temperature, Depth) and the turbidity probe (type: SeaPoint, STM), and 32 Hz for the flow probe. All datasets were recorded between September 17th 10:00 and September 25th 12:30. In this period a total number of 509 vessels passed the cross section. Observed parameters are exemplarily shown in Figure 2 considering the passage of one individual vessel. The grey dashed line is located at time step 120 s, a relative time with respect to the starting point of the passage. This point was chosen as a common reference point for

all observed passages as follows: In the data preprocessing, times of individual ship passages were reduced in order to match the maximum trough to the reference point.
Additionally, the ship provided AIS-signal (Automatic Identification System) was also recorded containing all relevant information of the passing ship. More specifically, AIS data sets provide length, beam, draft, speed and course over ground together with the ship's name and identifier. Furthermore, soil samples were taken in the cross section to obtain reliable information on the mass fraction of the particle size distribution. In Table 1 the main grain diameters are listed which represent the majority of the soil in the observed cross section. Therefore our investigations focus on these grain diameters. For further details of the field campaign in the Kiel Canal refer to [18].

Table 1. Grain size distribution [21].

Class name	grain diameter [µm]	mass fraction [%]
Very fine sand	62-125	19.0
Fine sand	125-250	38.4
Medium sand	250-500	17.6
		∑ = 75.0

According to the characteristics of the Kiel Canal, a separation of the measurements in natural and ship-induced effects is not needed. Therefore, the investigations can directly be performed. This distinguishes the presented work from other analyses like e.g. in [6]. Furthermore, effects of the propeller on the sediment entrainment have been ruled out in this study, since it is not possible to separate the amount of the propeller in the given measurements. A principal model of the propeller related impact in the near field of a vessel is given in [18] while the effect of propeller wash is investigated in [27].

4 METHODS

Aiming at robust and reliable results, different samples were created by either applying two different criteria (sample 1) ensuring all passages being independent and unaffected or also a third criterion (sample 2) intended to reduce the spatial influence of the observed parameters. Specifically, the criteria were as follows:

- the interval between consecutive ship passages (2 minutes before and 10 minutes after the reference point),
- the availability of the AIS-signal for the individual recorded ship passages,
- the distance of the individual recorded ship passages from the nearest probe (±2 m).

Since sample 1 is used for a correlation analysis, sample 2 is used for smoothing the turbidity record as well as for investigations concerning the critical grain diameter. The reason for using two different samples is that the absolute values of the measured parameters decrease with increasing distance to the probes as shown in Figure 3. The example shows how the fluctuation in the water level develops from the middle of the cross section to the southern canal bank. In this case, the vessel directly passed over the probe in the middle of the cross section (distance between ship's axis and probe 3 <5 cm) thus it can be assumed that the surface elevation is fully formed.

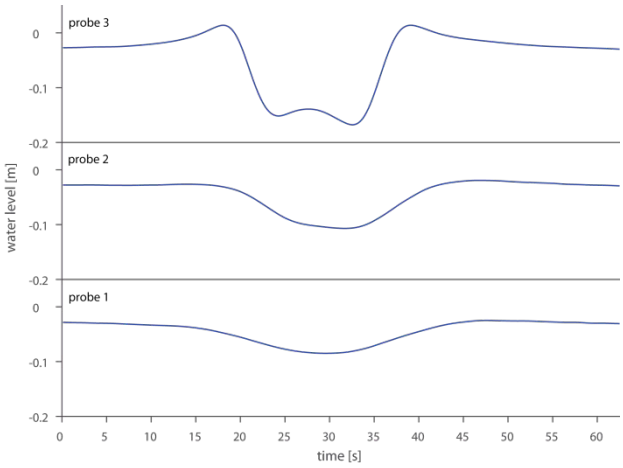

Figure 3. Development of the fluctuation in the water level from the middle of the cross section to the southern bank.

For the correlation analysis the absolute values of the parameters are less important because these analyses aim at describing the linear relationship between two recorded parameters as the tendency to move in the same/different direction. This is different when looking at the critical grain diameter which is estimated based on the smoothed turbidity records. Here, the absolute values of the time series are more important to examine the ship-induced amount of sediment in the water column. A drawback, however, is a reduced size of sample 2 compared to sample 1.
Before investigating the turbidity records in detail, some previous analyses need to be performed. In a first step, correlation coefficients between relevant parameters are computed. Detecting the relevant parameters is mainly based on the observational records. Therefore, available vessel parameters like speed over ground, length, beam, draft, submerged main section of the ship, and the blocking coefficient are taken into account. The blocking coefficient combines ship and waterway parameters to account for the interaction between the vessel and the characteristics of the observed cross section. The coefficient is defined as the submerged main section of the ship divided by the cross sectional area of the waterway at the observed site.
Further parameters are related to the primary wave system. The focus is on the three main values bow wave, drawdown, and stern wave. Also the maximum resulting flow velocity components (x, y, z direction) and the recorded turbidity maximum are considered.
The correlation coefficient R between two recorded parameters is defined as

$$R = \frac{C(x,y)}{\sqrt{C(x,x)\cdot C(y,y)}} \quad (1)$$

where C is the covariance which is defined for two random variables x and y as

$$\mathrm{Cov}(x,y) = \frac{1}{n-1}\sum_{i=1}^{n}(x_i - \mu_x)\cdot(y_i - \mu_y) \quad (2)$$

where n is the length of x and y and μ is the mean of x and y. Thus, the correlation coefficient ranges from -1 to 1, whereas correlation coefficients below zero show negative correlation, correlation coefficients equal to zero point out no correlation, and correlation coefficients larger than zero reveal a positive correlation.
The significance test is based on an approximate test for the hypothesis of no correlation. The estimation uses

$$p = |R|\sqrt{\frac{n-2}{1-R^2}} \quad (3)$$

and compares p with critical values from the t-distribution with n-2 degrees of freedom [22]. The critical values are chosen on a significance level of 5% which means, if $p \leq 0.05$, the correlation is significant.
In the next step two smoothing methods, namely moving average and principal component analysis (PCA), were tested and applied to the turbidity records of sample 2. The smoothing is required as the high frequency turbidity records also include spikes and outliers which need to be eliminated for further analyses. Additionally, some of the smoothing techniques enable to extract a common signal from likewise ship passages needed to describe the general system behavior. The results are later on used to derive a generalized and robust description of the high-resolution turbidity data and to avoid misinterpretations in the temporal location and/or in magnitude of the detected maximum.
The moving average (also called running mean) is an example for a low-pass filter technique removing higher frequencies from time series and thus smoothing the data. This method as well as other linear smoothing methods is reviewed in [23]. During the procedure, every n^{th}-value of the original time series Y is substituted by the mean of the n^{th}-value, the q previous and the q subsequent values of Y:

$$X_n = \frac{1}{2q+1}\cdot\sum_{j=-q}^{+q} Y_{n-j} \quad (4)$$

The successive calculation of the mean for all values of Y with a moving window of 2q+1 values that is continuously pushed forward is responsible for the method's name. The smoothing intensity can be controlled by changing the window size. A larger q leads to a larger window and therefore to a stronger decrease in the variance of Y. A disadvantage in this context is the missing availability of smoothing several data sets simultaneously. Each time series has to be smoothed individually.
In contrast, the PCA is a multivariate statistical method to detect the common signals in multidimensional data sets like a set of turbidity time series. The main advantage in this context is the possibility of identifying patterns in the data set. This allows showing up the similarities as well as the differences. Furthermore, the dimensions of the original dataset can be reduced by discarding certain information [24]. However, vessels with identical characteristics can be classified and then subsequently analyzed in groups.
[25] give a short description on how to use the PCA approach. The first step is the calculation of the eigenvalues and the eigenvectors of the covariance matrix. This builds a decomposition of the data set into orthogonal components based on the criterion of maximum variability. The eigenvectors are composed by one component for each dimension of the data set respectively (in this case turbidity time series for each vessel). Furthermore, the eigenvectors represent the principal components while the corresponding eigenvalues constitute the proportion of the total variance explained by the individual principal components. The original set of time series can be reconstructed by taking all the principal components into account. If the aim is to reduce the vessel's turbidity time series to the main common signal, not all principal components should reasonably be used for the analyses but these which explain most of the variance in the turbidity records.
The smoothed time series of the turbidity records will be used for investigating the relationship between ship-induced stress and the turbidity. In particular, the turbulent flow velocity at the bottom of the cross section is regarded to determine the entrainment of the sediments and the resuspension process. To get a first idea, a grain-diameter-based Froude number is used for the analyses [26]:

$$360 = \frac{v_m^2}{d_{crit}\cdot g} \quad (5)$$

where v_m is the mean velocity of the flow at the bottom of the cross section, d_{crit} is the critical grain diameter, and g is the gravitational acceleration. As mean flow velocity at the bottom of the cross section, the resulting ship-induced flow velocity at the bottom of the cross section is used. Hence, the results may be considered as approximation to describe the interaction between a passing ship and the waterway even if there are more detailed approaches for calculating the entrainment of the sediments.
Afterwards a threshold classification based on the critical grain diameter was conducted yielding in a general description of the turbidity curve for each group. In the last step, the groups are assigned to directly measurable parameters e.g. to AIS data like the length or the draft of a ship.

5 RESULTS

5.1 DATA ASSIMILATION

The data assimilation was performed using the described criteria for selecting unaffected ship passages. After that 257 passages remain for sample 1 (correlation analysis)

and 54 for sample 2 (turbidity record smoothing, investigations concerning the critical grain diameter). In case of sample 1, 195 of the 257 ships have been maneuvered above probe 3 in the center of the canal, 61 over probe 2 and 1 over probe 1 located close to the southern bank.

5.2 CORRELATION ANALYSIS

The results of the correlation analysis based on 257 recorded vessels are shown in Figure 4. The outcome is provided as matrix giving a quick overview of the selected parameters each of which is briefly characterized below. Correlations between individual parameters are shown as circles with the correlation coefficient inside. If the calculated correlation is not significant, the circle is drawn in white color. Otherwise, the circle is colored ranging from -1 (light green) to 1 (red) depending on the value of the correlation coefficient.
The correlation analysis indicates low or no significant correlations for the speed over ground with all other parameters since most ships passed with a speed of approximately 15 km/h, the official maximum speed in the Kiel Canal for all vessels. In contrary to that, strong dependencies are found between the ship's geometry and parameters of the primary wave system. This can be seen, in particular, in the draft and the drawdown ($R = 0.80$). The same is valid for the correlation between the maximum resulting flow velocity and the drawdown/draft ($R = 0.88/R = 0.82$). It is thus concluded that the maximum resulting flow velocity can be used for the characterization of a specific vessel. The maximum recorded turbidity shows significant correlations with almost all parameters but coefficients are rather small ($R < 0.35$) in contrast to the correlation between other parameters. Similar results for the correlations were found by [29] and further on used to predict ship-induced wave heights with empirical formulas. Regression analyses were performed as well to predict the maximum turbidity based on the bed shear stress.

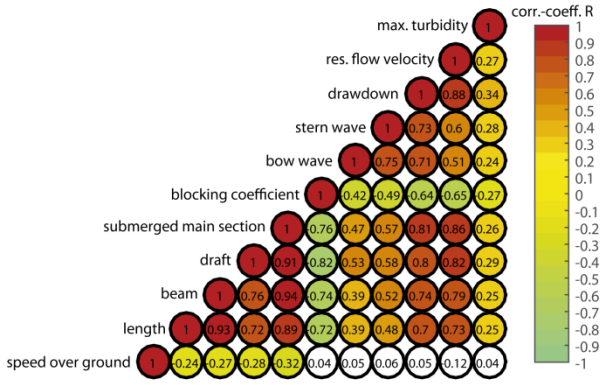

Figure 4. Correlation analysis.

A preliminary conclusion here is that the maximum turbidity also cannot be directly described by the chosen parameters. Furthermore, the maximum turbidity is probably not the ideal parameter for characterizing the turbidity records because of the complex physical ship/waterway-interaction and the fluctuations in the measurements due to the high frequency recording. Therefore, another method is introduced in the next chapters.

5.3 SMOOTHING TECHNIQUES

The correlation analysis above highlighted that the maximum recorded turbidity cannot be used to properly describe the entire ship-induced turbidity. A possible reason is the high sampling rate of 8 Hz. Infrequent outliers lead to a misinterpretation in temporal location and/or absolute value of the detected maximum. Figure 5 shows four arbitrary examples for those cases.

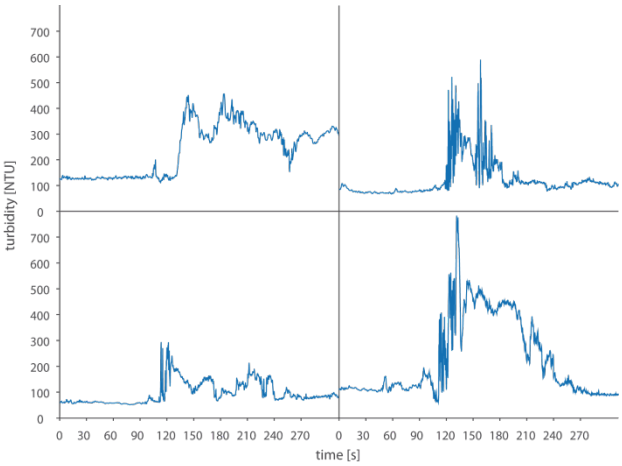

Figure 5. High frequency turbidity records.

Therefore, only the first and the second principal component were used to compress the information in the vessel's turbidity time series for the analyses. This enables to explain approximately 75 % of the variability of the turbidity records regardless of the sample. Each remaining principal component does not exceed 10 %.
Figure 6 finally summarizes the results of the smoothing techniques applied to two different turbidity records. The grey line in the background shows the observed high frequency turbidity time series. The red line is the moving average with a window size of 10 s (assumed to be appropriate for this issue without losing too much information but gaining a good result in smoothing at the same time) and the black line represents the reconstruction of the turbidity records based on the first and second principal component of sample 2 with 54 measurements of unaffected ship passages. The explained variance sums up to 76.4 % showing that only signals in the measurements have been removed that show strong individual characteristics of each vessel and of the prevailing environmental conditions during the vessel passage.
Figure 6 essentially shows the advantages and disadvantages of the applied methods. While the moving average fits very well to the original data, the PCA-approach shows a more general description. This fact is owed to the mathematical background of the methods. The moving average shows better results with increasing window sizes. Downside is the loss of information about the actu-

ally recorded peak. Contrary, this loss is much smaller when using the PCA. However, the detailed description is less good.
Since the following investigations focus on the general characteristic and on describing the peak values, the PCA-approach is used in the next chapter.

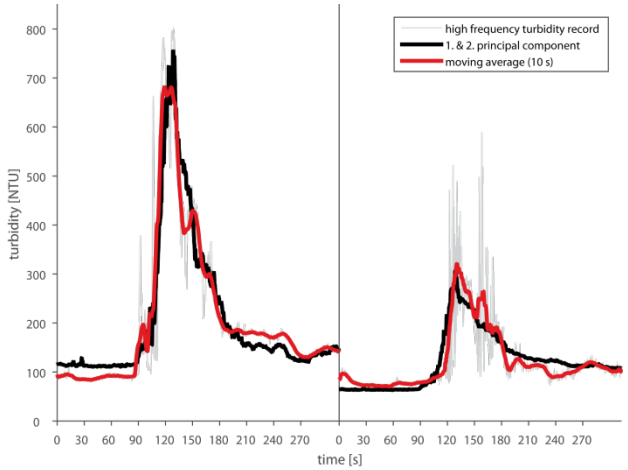

Figure 6. Summarized smoothing techniques.

5.4 CRITICAL GRAIN DIAMETER

The results of the grain diameter analyses are shown in Figure 7 for two exemplarily chosen vessels representing two different cases. The graphs are divided in two subplots. The upper plot shows the (calculated) critical grain diameter for each time step using equation (5) based on the flow velocity at the bottom of the cross section. The color shaded areas are classified by the grain diameters considering very fine sand, fine sand, and medium sand. The lower subplot shows the recorded high frequency turbidity in black as well as the first and second principal component reconstruction in red taking 54 measurements of unaffected ship passages (sample 2) into account.

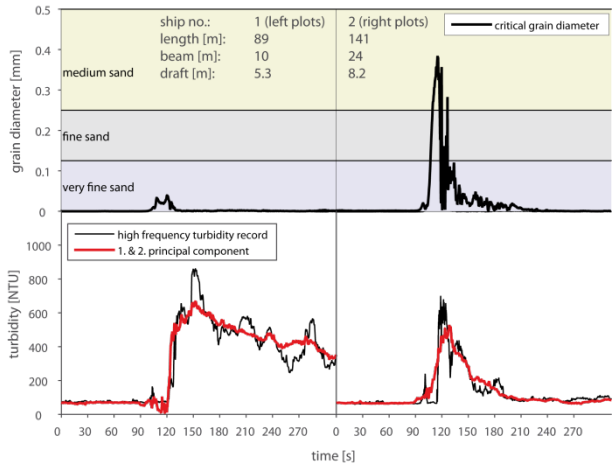

Figure 7. Recorded turbidity and calculated grain diameter.

However, the two different turbidity records in Figure 7 still have characteristics in common. Both time series in the lower part of the figure show a basic turbidity around 100 NTU. Due to the passing ship the turbidity quickly increases and reaches a maximum just after the occurrence of the trough (reference point at 120 s). Afterwards, the turbidity decreases until reaching the basic concentration again. The main difference in the shown examples is the time the turbidity remains in the water column. The critical grain diameters, shown in the upper subplots, allow for linking the different residence times to the flow velocity. As figured out on the left, the turbidity decreases slowly (consequently the residence time is long) in case that the recorded flow velocity at the bottom does not exceed the first threshold. The critical grain diameter shows that the recorded velocity only has the ability to resuspend very fine sand. In contrast to this, the turbidity decrease is much faster (therefore the residence time is short) in case that the flow velocity is large enough to resuspend medium sand, as shown by the large critical grain diameter. The physical background of the described behavior can only be assumed since the available measurements only provide information about the sediments on the canal bed and not about the sediment distribution in the water column. First, the different densities of the sediment fractions may impact the residence time. Medium sand with a higher density sinks faster than very fine material with a lower density. Another additional explanation for the shorter residence time in case that medium sand was resuspended might be that fast sinking grains affect slowly sinking particles and increase their sinking speed. As mentioned before, a verification of these explanations requires further but actually not available information.
Nevertheless, the critical grain diameter was mainly used as auxiliary parameter to classify the observed 54 vessels for further investigations. Since the shown behavior was found for all turbidity time series, this approach constitutes an appropriate classification methodology, regardless of the detailed allocation of the physical processes. Therefore, three classes were set up using the grain diameters as class limits as shown in Table 2. The individual time series were classified according to the maximum critical grain diameter.

Table 2. Classification based on the grain diameter.

Class name	range [mm]	number
Grain group 1	≤0.125	24
Grain group 2	>0.125 ≤0.250	16
Grain group 3	>0.250	14

In Figure 8 three subplots of the specific grain groups are shown. The gray marked lines in the background show the first and second principal component of the individual turbidity time series in the individual grain groups. The black line represents the mean time series of all ships in that group and the red shaded area highlights the standard deviation of each time step. Noticeable is the characteristic behavior which was already shown in Figure 7. Here the mean time series show the same behavior: ship passages that induced a rather small flow velocity at the canal bed were assigned to group 1 which shows a

low sink rate resulting in a long residence time. In contrast all ships that induced a rather high flow velocity were assigned to group 3 which shows a characteristic fast decrease of turbidity resulting in a shorter residence time. Another point is that, regarding the mean time series the maximum turbidity increases with the group number. This is shown better recognizable in Figure 9 where the three mean time series are plotted one upon the other.

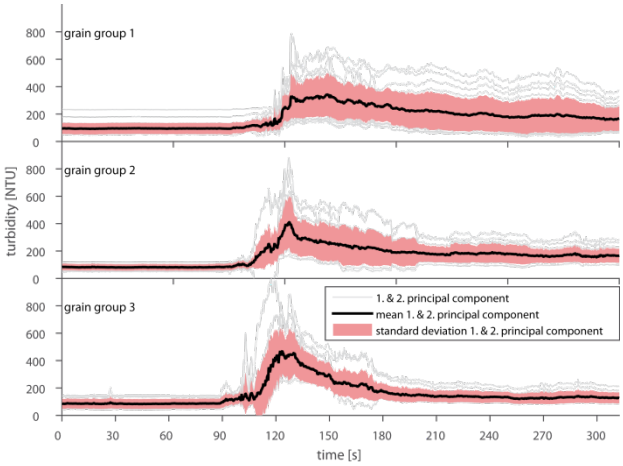

Figure 8. Mean turbidity of the grain groups including the standard deviations.

Furthermore, individual time series of a group have been tested for a systematic behavior, e.g. checking all time series that tend to be higher than the group mean for exceeding a certain draft. These tests did not show up any dependencies and clarify that the ship-induced sediment resuspension is a complex physical process which cannot be linked to single parameters. Sediment behavior like flocculation as well as environmental effects in the particular waterway cross section affects the results.

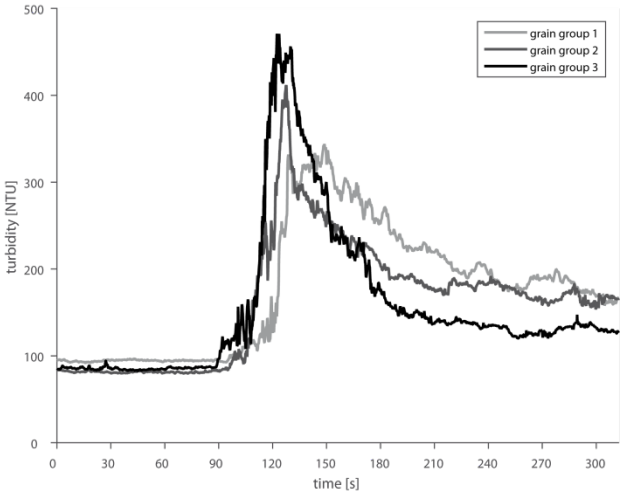

Figure 9. Mean turbidity of the grain groups.

However, for the given section of the Kiel Canal the described classification approach allows splitting the given data set of observed ship passages based on the critical grain diameter resulting in three groups, each with a characteristic behavior and a significant difference in turbidity residence time. The three groups are shown in Figure 9, the black time series marks the development of grain group 3, the dark grey line of grain group 2 and the light grey line of grain group 1.

With the flow velocity at the canal bed, the chosen classification needs a parameter which is usually not available. Therefore the next step considers permanent available ship parameters like the AIS-data. Furthermore, it is necessary to quantify the uncertainties in terms of the spread around the mean values in this case with the standard deviation. Figure 10 shows four parameters and their distribution over the three grain groups exemplarily. The mean is displayed as a red line, the blue box around the mean represents the spread in terms of the standard deviation and the horizontal black lines below and above the box are the minimum and maximum of each parameter. The plot clearly shows a strong dependency between the parameters and the grain groups. The larger the resuspended grain diameter, the larger are the mean parameters. Except for the flow velocity the spread decreases with an increasing grain group. The strong dependency between the resulting flow velocity at the bottom and the grain groups results from calculating the critical grain diameter on base of the flow velocity. Here, the range of the flow velocities assigned to each grain group representing an idealized characteristic of the turbidity should be shown. However, same results are valid for other parameters not shown in Figure 10.

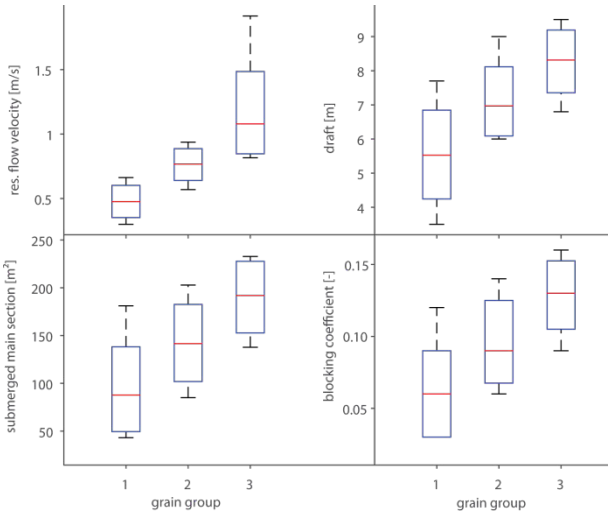

Figure 10. Grain groups vs. ship parameters.

6 CONCLUSIONS

In this paper, a field campaign in the Kiel Canal was evaluated. The analyses have been performed during a joint research project between the German Federal Waterways Engineering and Research Institute and the Research Institute for Water and Environment of the University of Siegen. Strong dependencies between the ship's geometry and the primary wave system parameters or the maximum resulting flow velocity at the bottom of the cross section were identified. However, the correlation analysis also revealed that the turbidity is a highly sensitive parameter requiring higher effort to be de-

scribed compared to e.g. afore mentioned parameters. Therefore, the principal component analysis was used to find out common patterns in the turbidity measurements. The common signal in the turbidity records in terms of the first and second principal component were used to link a critical grain diameter and the corresponding flow velocity at the bottom of the cross section. This approach was used to classify the turbidity records and not to describe the underlying physical processes in detail. The classification shows appropriate results and can additionally be directly assigned with AIS-transmittable parameters (e.g. length or draft of a ship). A validation of the chosen grain diameter approach is still needed and should include comparisons with other studies. Thresholds of sediment movement are e.g. described by [28].

In a next step, further effort is on deriving a generalized description of the classified turbidity time series since the high resolution records still contain individual characteristics. On this basis, the maximum but also the total shape of the generalized turbidity curves can be taken into account depending on the specific issue. An estimation of the ship-induced sediment transport will then be possible with the residence time from the generalized turbidity time series (assuming a higher amount of suspended sediment concentration during the residence time). The proportion of ship-induced sediment transport including uncertainties can then be approximated for waterways based on AIS-transmitted parameters.

Furthermore, combined with AIS-parameters a future sediment transport can also be estimated based on the expected ship traffic.

However, the current results are still limited to the Kiel Canal. To achieve a general description of the sediment transport the developed methods have to be applied to other (tidal) waterways, e.g. the Elbe river.

7 ACKNOWLEDGEMENTS

The shown analyses are derived from the research project "Schiffserzeugter Sedimenttransport an Seeschifffahrtsstraßen (SeST)" funded by the German Federal Waterways Engineering and Research Institute (BAW). The authors of the Research Institute for Water and Environment at the University of Siegen are grateful to the corresponding personnel at the BAW who are also co-authors of this paper and who run the field measurements, prepared and provided the large variety of data as well as helpful comments within the research project.

8 REFERENCES

1. Barnard, P.L.; Schoellhamer, D.H.; Jaffe, B.E.; McKee, L.J. (2013). Sediment transport in the San Francisco Bay Coastal System: An overview, *Marine Geology* 345: pp. 3-17. doi:10.1016/j.margeo.2013.04.005.

2. Simons, D.B.; Sentürk, F. (1992). Sediment Transport Technology: Water and Sediment Dynamics, *Water Resources Publication*, Colorado, USA.

3. Johnson, J.W. (1957). Ship waves in navigation channels, *Proceeding of the 6th coastal Engineering Conference*, Gainesville, Florida. ASCE: pp. 666–690.

4. Schoellhammer, D.H. (1996). Anthropogenic sediment resuspension mechansim in a shallow microtidal estuary, *Estuar. Coast. Shelf Sci.* 43: pp. 533-548. doi:10.1006/ecss.1996.0086.

5. Houser, C. (2011). Sediment Resuspension by Vessel-Generated Waves along the Savannah River, Georgia, *Journal of Waterway, Port, Coastal, and Ocean Engineering* 137: pp. 246-257. doi:10.1061/(ASCE)WW.1943-5460.0000088.

6. Rapaglia, J.; Zaggia, L.; Ricklefs, K.; Gelinas, M.; Bokuniewicz, H. (2011). Characteris-Tics Of Ship's Depression Waves And Associated Sediment Resuspension In Venice Lagoon, Italy, *Journal of Marine Systems* 85: pp. 45-56. doi:10.1016/j.jmarsys.2010.11.005.

7. Rapaglia, J.; Zaggia, L.; Parnell, K.; Lorenzetti, G.; Vafeidis, A.T. (2015). Ship-wake induced sediment remobilization: Effects and proposed management strategies for the Venice Lagoon, *Ocean & Coastal Management* 110: pp. 1-11. doi:10.1016/j.ocecoaman.2015.03.002.

8. Ji, S.; Ouahsine, A.; Smaoui, H.; Sergent, P. (2014). 3D Modeling of sediment movement by ships-generated wakes in confined shipping channel, *International Journal of Sediment Research* 29: pp. 49-58. doi:10.1016/S1001-6279(14)60021-4.

9. Madsen, P.A.; Sørensen, O. (1992). A new form of Boussinesq equations with improved linear dispersion characteristics. Part 2. A slowly-varying bathymetry, *Journal of Coastal Engineering* 18: pp. 183-204. doi:10.1016/0378-3839(92)90019-Q.

10. Dam, K.T.; Tanimoto, K.; Nguyen, B.T.; Akagawa, Y. (2006). Numerical study of propagation of ship waves on a sloping coast, *Journal of Ocean Engineering* 33: pp. 350-364. doi:10.1016/j.oceaneng.2005.05.003.

11. Sorensen, R.M. (1997). Prediction of vessel-generated waves with reference to vessels common to the upper Mississippi river system, *Technical report*, Department of Civil and Environmental Engineering, Lehigh University, Bethlehem, PA, USA.

12. Krey, K. (1913). Fahrt der Schiffe auf beschränktem Wasser, *Schiffbau* 14.

13. Dand, J.W.; White, W.R. (1978). Design Of Navigation Canals, *Symposium on aspects of navigability of constraint waterways including harbour entrances*, Delft, Netherlands.

14. Jensen, J.; Kelln, V.; Niehüser, S.; Uliczka, K.; Kondziella, B. (2015). Entwicklung empirisch-analytischer Ansätze als Proxy für schiffserzeugten Sedimenttransport an Seeschifffahrtsstraßen, *HTG Kongress 2015*, Bremen, Deutschland, HTG: pp. 231-240.

15. Jensen, J. (1998). Ermittlung von schiffserzeugten Belastungen an Wasserstraßen, *Tagungsband Numerische Verfahren in der Wasserbaupraxis*, Verein zur Förderung der wissenschaftlichen Weiterbildung an der Universität-Gesamthochschule Siegen e.V. (fww): pp. 125-136.

16. Bertram, V. (2000). Practical ship hydrodynamics, *Butterworth-Heinemann*, Oxford, UK.

17. BAW (2006). Anpassung der Fahrrinne von Unter- und Außenelbe an die Containerschifffahrt, *Gutachten zu den ausbaubedingten Änderungen der schiffserzeugten Belastung*, (BAW-Nr. A3955 03 10062).

18. Uliczka, K.; Kondziella, B. (2016). Ship-induced sediment transport in coastal waterways (SeST), *Proceedings of 4th MASHCON*, Hamburg, Germany. (submitted).

19. Brockmann, J.; Heeling, A.; Pohl, P.; Uliczka, K. (2008). The Kiel Canal (Nord-Ostsee-Kanal), *Die Küste* 74: pp. 317-332.

20. Thormählen, C. (2010). Modernisation of the Brunsbüttel locks, *PIANC Yearbook* 2010: pp. 131-134.

21. Aqua Vision BV (2012). Suspended sediment measurements in the Kiel Canal. *Report AC_DOC_120149 Concept*, Utrecht, Netherlands. (unpublished).

22. Von Storch, H.V.; Zwiers, F.W. (1999). Statistical analysis in climate research, *1st edn. Cambridge University Press*, Cambridge, UK.

23. Buja, A.; Hastie, T.; Tibshirani, R. (1989). Linear smoothers and additive models (with discussion), *The Annals of Statistics* 17: pp. 453–555. URL:http://www.jstor.org/stable/2241560.

24. Smith, L.I. (2002). A tutorial on Principal Components Analysis, *Cornell University*, USA.

25. Marcos, M.; Gomis, D.; Monserrat, S.; Alvarez-Fanjul, E.; Perez, B.; Garcia-Lafuente, J. (2005). Consistency of long sea-level time series in the northern coast of Spain, *Journal of Geophysical Research* 110: C03008. doi:10.1029/2004JC002522.

26. Kresser, W. (1964). Gedanken zur Geschiebe- und Schwebstofffführung der Gewässer, *Österreichische Wasserwirtschaft* 16: pp. 6-11.

27. Williams, R.; Wang, T.; Whelan, M.; Shepsis, V.; Poon, Y. (2006). Methodology for estimating effects from propeller wash: Case Studies, *Poster Session No. 50, 30th ICCE*, San Diego, California, USA.

28. Komar, P.D.; Miller, M.C. (1973). The threshold of sediment movement under oscillatory water waves, *Journal of Sedimentary Petrology* 43: pp. 1101−1110.

29. Göransson, G.; Larson, M.; Althage, J. (2014). Ship-Generated Waves and Induced Turbidity in the Göta Älv River in Sweden, *Journal of Waterway, Port, Coastal, Ocean Engineering*: doi:10.1061/(ASCE)WW.1943-5460.0000224.

9 AUTHORS' BIOGRAPHIES

Sebastian Niehüser, M.Sc., is the lead author of this paper and research associate of the Research Institute for Water and Environment at the University of Siegen. He is responsible for engineering as well as research projects in the field of extreme value analysis, probabilistic methods and flooding risks at coastal and inland sites. Since 2014 he is working on issues in relation to the interactions between the ship-induced stress and the corresponding sediment transport within the research project SeST.

Marius Ulm, M.Sc., is a research associate at the Research Institute for Water and Environment of the University of Siegen. He is responsible for research and engineering projects in the field of coastal and inland hydraulic engineering. In particular, he is mainly involved in the SeST research project from which the presented outcomes result from. His previous experience includes data and time series analysis as well as numerical modeling.

Arne Arns, Dr.-Ing., is employed at the Research Institute for Water and Environment (fwu) of the University of Siegen. He is currently Research Fellow and team leader of the coastal extremes group. He has experience in publishing scientific results, teaching, engineering and applying for, working on, and coordinating research projects.

Jürgen Jensen, Prof. Dr.-Ing., has a full professorship in Hydraulics, Hydraulic Structures and Coastal Engineering at the University of Siegen and is head of the Research Institute Water and Environment (fwu). His experience ranges from coastal engineering, probabilistic and statistical methods, physical and numerical models for the optimization of hydraulic and coastal structures to ship waves and interactions with the waterways.

Vitalij Kelln, Dipl.-Ing., holds the current position of a research associate at the Research Institute for Water and Environment (fwu) at the University of Siegen. He is responsible for the research project SeST, hydraulic engineering projects, and teaching of hydrodynamic numerical modeling. His previous experience includes

time series analysis, extreme value statistics, and hydrodynamic numerical modeling.

Klemens Uliczka, Dr.-Ing., holds the current position of Senior Research Engineer at the Federal Waterways Engineering and Research Institute (BAW), Hamburg Office, Germany. He is responsible for the task of interaction ship/waterway at the coastal department. His previous experiences include coastal engineering, tidal dynamic in estuaries and design of banks and revetments at approach channels.

Bernhard Kondziella, Dipl.-Ing (FH), holds the current position of Research Engineer at the Federal Waterways Engineering and Research Institute (BAW), Hamburg Office, Germany. He runs investigations about the interaction ship/waterway at the coastal department and since 2011 he is responsible for the field measurements in the research project SeST. His previous experiences include model and field measurements in estuaries and approach channels.